Aerosol Science and Technology

ISSN: 0278-6826 (Print) 1521-7388 (Online) Journal homepage: http://www.tandfonline.com/loi/uast20

Monitoring Motor Vehicle PM Emissions: An Evaluation of Three Portable Low-Cost Aerosol Instruments

M. Matti Maricq

To cite this article: M. Matti Maricq (2013) Monitoring Motor Vehicle PM Emissions: An Evaluation of Three Portable Low-Cost Aerosol Instruments, Aerosol Science and Technology, 47:5, 564-573, DOI: 10.1080/02786826.2013.773394

To link to this article: http://dx.doi.org/10.1080/02786826.2013.773394

Aerosol Science and Technology, 47:564–573, 2013

ISSN: 0278-6826 print / 1521-7388 online
DOI: 10.1080/02786826.2013.773394

Monitoring Motor Vehicle PM Emissions: An Evaluation of Three Portable Low-Cost Aerosol Instruments

M. Matti Maricq
Research & Advanced Engineering, Chemical Engineering Department, Ford Motor Company, Dearborn, Michigan

The burgeoning diversification of particulate matter (PM) emissions regulations creates the need for aerosol monitors for use in engine development, on-board PM measurement, off-road emissions testing, roadside monitoring, and other applications where conventional instruments are impractical or too costly. This work critically examines from two perspectives the performance of three small, relatively inexpensive devices, the DustTrak, Pegasor Particle Sensor, and Diffusion Size Classifier, in engine exhaust PM measurement. First, results from chassis dynamometer vehicle emissions testing reveal that all three can provide accurate PM data that correlate well with the regulatory methods for PM mass and number, but only when there is little variation in morphology and composition. Second, detailed laboratory characterizations with oil and soot aerosols are reported that elucidate how these devices respond to particle size, morphology, and composition. They show that changes in aerosol properties affect all three monitors, but to a degree that depends on their particular detection method, optical, electrical charging, and charging plus diffusion. The results provide calibration data and describe conditions under which these monitors can reliably record PM emissions from engine exhaust.

[Supplementary materials are available for this article. Go to the publisher's online edition of *Aerosol Science and Technology* to view the free supplementary files.]

INTRODUCTION

Concerns about potential health effects and reductions in legislated emissions standards have focused considerable attention on particulate matter (PM) emissions from motor vehicles over the past two decades. Presently, California passed LEV III revisions, the PM portions of which are to begin phase-in starting with the 2017 model year, and the US Environmental Protection Agency (EPA) is writing similar Tier 3 standards. With Stage 6, the European Union will extend the solid particle number standard to include gasoline direct injection technology. The stringency of these standards (3 mg/mile, in US, and 6×10^{11} particles/km, in EU) is such that virtually all motor vehicles will require PM testing during research and development to ensure they meet certification. The increased testing burden cannot be met solely with existing tools.

Smoke meters (Homan 1985) have historically been used for engine development and the gravimetric filter method for vehicle certification. The increased attention on PM and tighter emissions standards have necessitated a migration to aerosol instruments, which are becoming more common in automotive research and advanced development laboratories to make real-time measurements of particle number, size, and mass. But there are many other areas of motor vehicle development that will require, or benefit from, PM data, including durability testing, verification of on-board diagnostics, on-road emissions testing, production line quality checks, inspection and maintenance, and so forth. Smoke meters are not sufficiently sensitive at the new emissions levels, research and development instruments are too complex and costly, and regulatory methods are too complex, costly, and impractical, e.g., the need to weigh filters for gravimetric mass. This situation is not unique to motor vehicles; e.g., the need for suitable sensors applies as well to diesel exhaust exposure in mines (Cauda et al. 2012) and workplace exposure to engineered nanoparticles (Wiesner et al. 2006).

Current commercially available aerosol instruments for emissions testing tend to be higher-end devices aimed at recording particle size distributions and second-by-second PM mass and number. The smoke meter provides a simple reading of relative opacity, but has the distinct advantage of simplicity and the robustness to measure PM directly from raw exhaust. There are a variety of aerosol sensors and monitors (Burtscher, 2005) that can potentially supplant the smoke meter. Some have been investigated and used for engine exhaust PM, such as diffusion chargers (Bukowiecki et al. 2002; Ntziachristos et al. 2004; Jung and Kittelson 2005) and a nephelometer (DustTrak) (Moosmüller et al. 2001; United States Environmental Protection Agency

Received 12 December 2012; accepted 26 January 2013.
The author is grateful to Joseph Szente, Mike Loos, Lora Kralik, and Amy Harwell for their help with the array of PM measurement during vehicle emissions testing. The author also thanks Martin Fierz, Heinz Burtscher, Kauko Janka, Juha Tikkanen, and Leonidas Ntziachristos for helpful discussions about the DiSC and PPS.
Address correspondence to M. Matti Maricq, Research & Advanced Engineering, Chemical Engineering Department, Ford Motor Company, MD 3179, P.O. Box 2053, Dearborn, MI 48121, USA. E-mail: mmaricq@ford.com

2008). In addition, new devices continue to be developed, including the recent Pegasor Particle Sensor (PPS) (Lanki et al. 2011; Ntziachristos et al. 2011) and diffusion size classifier (DiSC) (Fierz et al. 2008a, 2011) examined in the present work. These are likewise diffusion-charger-based but add new twists; the PPS is designed for raw tailpipe measurements and the DiSC incorporates particle-sizing capability.

The present aim is to evaluate the performance of these two new PM monitors, as well as the DustTrak, for engine exhaust applications, the latter because it has seen some success in this use and offers an instructive contrast in detection principle. Such evaluations are often carried out by simultaneously sampling diluted engine exhaust with an array of test instruments, and grading performance by how well they agree with the gravimetric method (Mohr et al. 2005; Liebowitz and Hansen 2011). This can quickly identify suitable candidates, but suffers the limitation that one cannot extrapolate performance to situations outside of the test matrix. Thus, the present article takes a two-step approach. First, we examine performance on vehicle exhaust over the regulatory Federal Test Procedure (FTP), where agreement is good, and the US06 drive cycle, where it is not. Second, we examine monitor response to oil and soot aerosols, with the idea that composition-wise, these represent the two extremes of engine exhaust particles.

EXPERIMENTAL METHODS

Chassis Dynamometer Testing

Test vehicles are run on a 48" single-roll electric chassis dynamometer. The exhaust is sampled through a full-flow constant volume sampling (CVS) dilution tunnel. Dilution occurs approximately 1 m behind the tailpipe using a "remote mix tee." The dilution air is taken from the test cell, conditioned to 38°C and low humidity (–9°C dewpoint), and filtered (>90% removal). The diluted exhaust is transported to a stainless steel tunnel via a 25-cm diameter electrically conductive coated Teflon tube. Samples for filter collection and instruments are taken at more than 10 tunnel diameters downstream to allow complete mixing. This work employed CVS flow rates of 9.9 and19.8 m^3/min.

The instrument evaluation was conducted with five gasoline turbocharged direct injection (GTDI) development vehicles; four have 3.5 L engines (labeled A–E, with B and C repeat test series of the same vehicle) and one a 2.0 L engine. All are equipped with three-way catalysts. Certification test fuel was used, either E0 or E10 (0% and 10% ethanol in gasoline, respectively).

Six methods were used to record the mass and number of PM emissions, although not all in every test. Gravimetric PM mass is determined according to the Code of Federal Regulations 40 Part 1065 (United States Environmental Protection Agency 2011) using 47-mm-diameter Teflon filters. Elemental/organic carbon (EC/OC) analysis is done using quartz filters, and thermal analysis by a Horiba MEXA 1370PM. Total PM mass by this method has been found to agree well with the gravimetric method (Akard et al. 2004). Real-time PM mass is recorded by a Dekati mass monitor (DMM) (Lehmann et al. 2004). The solid particle (soot) mass is measured by a photoacoustic soot sensor (PASS) (AVL micro soot sensor) (Linke et al. 2004). Both total and solid particle number emissions are measured. The total number, greater or approximately equal to 10 nm, is sampled from the tailpipe using a three-stage ejector pump (first stage 190°C, second and third 23°C), diluted by ∼1000, and counted by a 3010 CPC (condensation particle counter). Solid particles greater than 23 nm are recorded from the CVS tunnel with an AVL particle counter according to the European Union Particle Measurement Program (PMP) (Giechaskiel et al. 2012). See the free online supplementary information for additional details.

Characterization with Laboratory Aerosols

Detailed instrument response is investigated with monodisperse and polydisperse oil and soot aerosols in the 20- to 300-nm mobility diameter range. The experimental setup is illustrated in the online supplemental information (Figure S1). Poly alpha olefin (PAO) oil droplets are generated via evaporation condensation. Soot particles are sampled from a rich premixed ethylene flame and allowed to grow by coagulation in a residence tube to a desired size. The size distributions are close to log-normal, with σ_g generally 1.4–1.5 for oil droplets and 1.5–1.7 for soot (Figure S2). Test aerosols are diluted to appropriate concentrations primarily using synthetic air, but in some experiments, N_2 is used to check if diluent choice affects DiSC or PPS operation.

To generate monodisperse particles, the oil or soot aerosol passes through a ^{210}Po neutralizer and differential mobility analyzer (DMA) to select particles within a narrow range of mobility diameter ($\sigma_g = 1.05$–1.1). The presence of multiply charged particles with the same mobility is minimized by ensuring the selected size exceeds the input aerosol mean diameter. The size-selected particles are distributed to the PM monitors, an electrometer, and a scanning mobility particle sizer (SMPS). The electrometer records particle number and the SMPS verifies the particles' monodispersity. A neutralizer is optionally placed upstream of the monitors to return the unipolar aerosol exiting the DMA to a Boltzmann charge distribution.

Experiments with polydisperse aerosols proceed in the same way but without a DMA for size selection. Test aerosols are sampled in parallel by the monitor(s) and the SMPS, with the latter used to provide the size and number of particles. The CPC used with the SMPS is calibrated against an electrometer, and particle losses are estimated and corrected using the TSI AIM software. With this, the polydisperse and monodisperse data are in good agreement, except for a ∼23% systematic offset (discussed in the online supplemental information).

TABLE 1
PM monitor specifications

Monitor	Principle	Sensitivity	Size	Response	Sampling
DustTrak II 8530	Light scattering	0.001–400 mg/m^3	0.1–10 μm	1 s	Dilute
Pegasor (PPS)	Electrical charge	0.001–250 mg/m^3	10–2500 nm	0.2 s	Raw or dilute
DiSCmini	Electrical charge	10^3–10^6/cm^3	10–500 nm	1 s	Dilute

MONITOR PRINCIPLES OF OPERATION

DustTrak II

The main features of the PM monitors are listed in Table 1. The DustTrak (TSI Model 8530) is a nephelometer that has seen widespread use in indoor air quality and occupational exposure applications (Lee et al. 2002; Seaton et al. 2004). The aerosol sample is drawn in at 3 L/min, with 1 L/min split off, filtered, and used as a sheath flow to protect the optics. Impactors can be used to preselect an upper size cutpoint, but were not employed in the present work. As the aerosol enters the detection volume, it intersects with a sheet of 780 nm laser light. Scattered light is collected by a gold mirror and directed to a photodetector at 90^o to the incident beam. The detector output is calibrated to PM mass using Arizona Test Dust (ISO 12103–1, A1 Test Dust). To avoid damage from water condensation and high temperature, the DustTrak can only be used with diluted exhaust gas.

PPS

The PPS records PM via diffusion charging. It works on the principle of escaping charge (Lehtimäki 1983; Lanki et al. 2011). The sample aerosol is drawn from the exhaust pipe by an ejector pump at an inlet flow of 2–8 L/min, as adjusted by the pressure of air or N_2 supplied. A corona discharge in the ejector produces ions, which attach to the entering particles as the ejector and inlet flows mix. A trap removes excess ions, but allows the charged particles to exit the sensor. The corona and trap are electrically isolated, except for one path through an electrometer; hence, any removal of charge by the exiting particles is detected as the return current needed to maintain charge conservation. This current is related to active surface area; so, auxiliary information, principally mean size, is needed to convert this to particle number or PM mass. However, the ability to monitor PM without the need to collect particles offers significant benefits in ease of use and maintenance. The PPS is designed to sample raw exhaust, in which case, it and the sample path must be heated, typically to ~190°C, and the sensor outlet is connected back to the exhaust pipe to mitigate the influence of exhaust pressure variations during transient operation. The PPS is not heated when measuring from the CVS tunnel.

DiSC

The Diffusion Size Classifier (miniDiSC) differs from other diffusion chargers by incorporating a diffusion stage (Fierz et al. 2008b, 2011). Entering particles are charged by a corona discharge, pass through an ion trap, a diffusion stage, and then a filter. The diffusion screens register a current from particles captured by diffusion, and the filter records the current imparted by the remaining particles. A time-varying aerosol generates an additional induced current from the net difference in particles entering and leaving at any given time. This is detected as the derivative of the filter current and subtracted from the diffusion stage to yield the net deposited current. The ratio of total to diffusion current is related to the mean mobility diameter, whereas the total current scales with particle number and size. By assuming a standard deviation, e.g., $\sigma_g = 1.7$ for engine exhaust particles (Harris and Maricq 2001), the DiSC can report real-time particle number concentration and mean diameter. The instrument is designed for ambient ultrafine particle measurement; thus, engine exhaust must be diluted to protect against high temperature and water condensation.

RESULTS

The results are divided into two parts. The first explores monitor performance on motor vehicle exhaust against the regulatory gravimetric filter PM mass and solid particle count methods, as well as DMM, photoacoustic, and thermal EC/OC measurements. Part two examines in detail how these monitors respond to particle size, composition, and electrical charge. Vehicle emissions data are described first to help motivate the need for a more detailed understanding of these monitors beyond how well they agree with regulatory methods.

Vehicle Exhaust PM

The PPS is designed to measure directly from raw exhaust, but the DustTrak and DiSC do not have this capability. Therefore, the results presented here are with all three instruments measuring diluted exhaust from a full-flow CVS tunnel. However, the results should be equally valid for partial flow dilution systems (Khalek 2007). PPS performance with raw exhaust is discussed in the online supplemental information.

Figure 1 compares second-by-second PPS and DustTrak measurements of PM emissions from a GTDI vehicle to the PM mass recorded by DMM during the cold-start phase of the

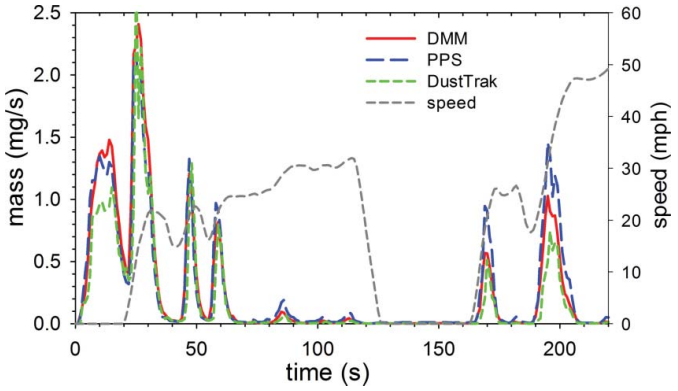

FIG. 1. PPS, DustTrak, and DMM measurement of transient PM mass emissions during a cold-start test of a 3.5 L GTDI vehicle. (Color figure available online.)

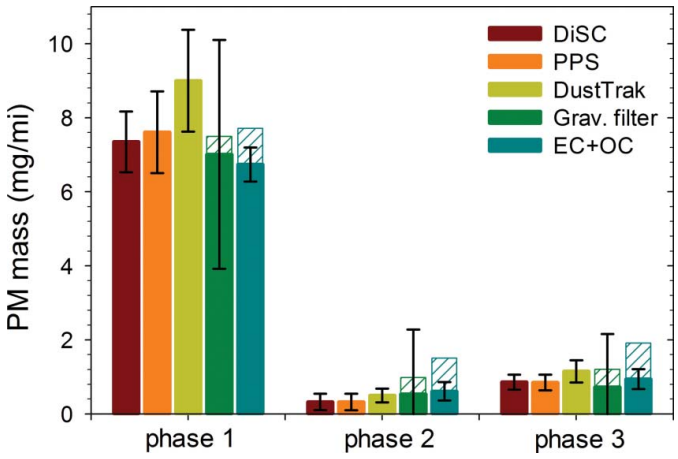

FIG. 2. DiSC, PPS, DustTrak, gravimetric filter, and EC + OC measurement of PM mass emissions for cold-start (phase 1), urban (phase 2), and hot-start (phase 3) portions of the FTP test. Plotted are the mean and $\pm 2\sigma$ error bars for four repeat tests of GTDI vehicle C. (Color figure available online.)

FTP drive cycle. The agreement between these monitors and DMM is quite good, with deviations in the peak emissions during vehicle acceleration generally within $\pm 20\%$. In raw exhaust measurement, the PPS's faster time response (0.2 s) would give sharper peaks than the DMM (1 s), but here, they are broadened from CVS dilution tunnel sampling. The performance in Figure 1 is encouraging, but not sufficient, since the DMM is not a reference standard. There exists no absolute calibration standard for PM; rather, for vehicle emissions, it is operationally defined by the EPA Part 1065 gravimetric filter method.

The DustTrak is factory-calibrated to mass, but the DiSC and PPS measure electrical currents from charged particles. These currents are converted to particle number concentration based on the size-dependent charging efficiencies reported in part two of the results, and then to mass. The first step requires knowing particle mean diameter and geometric standard deviation, whereas the second needs additional information on particle density. The DiSC determines size by its diffusion stage, but this must be assumed or measured separately for the PPS. Given number and size, the assumptions of a lognormal size distribution and power law effective density yield a PM mass

$$M = N_0 \frac{\pi}{6} \rho_0 d_0^{(3-D_f)} \mu_g^{D_f} e^{D_f^2 (\ln \sigma_g)^2/2}, \qquad [1]$$

where N_0 represents particle number, μ_g and σ_g are the geometric mean and standard deviation, ρ_0 and d_0 are the primary particle density and diameter, and D_f is the mass–mobility exponent for soot agglomerates. Many of these parameters vary only slightly as a function of fuel and engine type; typically, $\rho_0 = \sim 2$ g/cm^3, $d_0 = \sim 20$ nm, $\sigma_g = \sim 1.7$, and $D_f = \sim 2.3$, leaving particle number and size as the main factors determining PM mass (Maricq and Xu 2004). In the case of PAO oil droplets, $\rho_0 = 0.82$ g/cm^3, $D_f = 3$, d_0 is not needed, and $\sigma_g = \sim 1.5$.

Regulatory methods require PM collection over a defined drive cycle. Figure 2 displays results from four repeat tests of GTDI vehicle C over the three-phase FTP cycle, and Figures S3 and S4 corroborate these results for a larger number of vehicles. The three monitors give mass emissions in good agreement with two different filter methods, gravimetric and EC/OC. Calculation of PM mass from PPS data requires independent knowledge of particle size. Here, it is estimated from the ratio of particle mass to number via Equation (1) (e.g., PASS vs. solid particle count). For FTP phases 2 and 3, this yields mean diameters in the range of 75 ± 10 nm for these GTDI test vehicles; but during cold start, this can increase to $\sim$90 nm. DiSC mean diameter data (corrected for soot agglomerates) corroborate these estimates (Figure S6). For the filter-based measurements, full bar heights in Figure 2 represent the total material collected, whereas the hashed areas indicate nominal 5 and 10 μg contributions from gaseous adsorption artifacts for Teflon and quartz filters, respectively. It is worth noting in Figures 2 and S3 that measurement variability is comparable for the PM instruments and EC/OC analysis, but is about three times larger with the gravimetric method.

Figure 3 (and S5) compares DiSC- and PPS-derived particle number emissions to EU PMP-compliant solid particle and 3010 CPC total particle counts. DiSC and PPS results lie between the solid and the total particle data. Both devices are sensitive to all particles, not just solid ones, and extend below the PMP 23 nm cutpoint; thus, their exceedance of solid particle number is expected. Unlike the other instruments, the 3010 CPC sampled diluted exhaust at the tailpipe, decreasing by a few seconds the time available for particle coagulation. This and its lower size cutoff help explain why the 3010 CPC total particle count is higher than determined by DiSC and PPS. Measurement variability of DiSC particle number is comparable to the two counting methods. The PPS exhibits 2–3 times higher variability, but includes the uncertainty in correcting raw data for various trap voltage/flow rate settings examined for different tests.

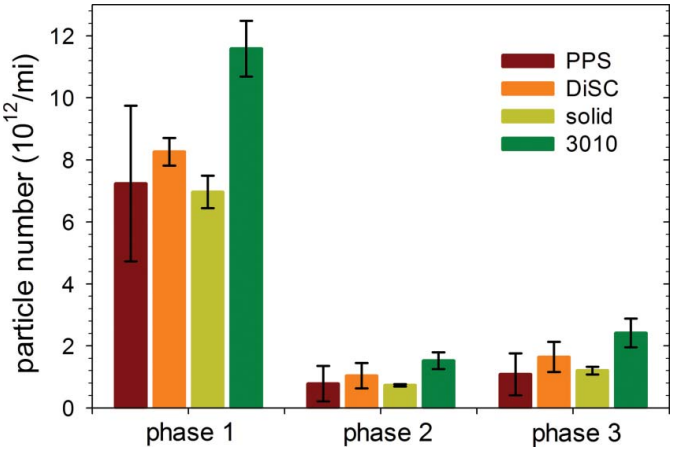

FIG. 3. PPS, DiSC, solid particle, and total particle (3010 CPC) measurements of particle number emissions for cold-start, urban, and hot-start portions of the FTP test. Plotted are the mean and $\pm 2\sigma$ error bars for four repeat tests of GTDI vehicle A. (Color figure available online.)

Whereas the FTP corresponds roughly to city driving, the US06 drive cycle was introduced to account for the higher speeds/loads associated with freeway driving. Figure 4 compares PM mass emissions recorded over this cycle. The test begins with generally good agreement between the four instruments, but midway into the high-speed portion, at ~340 s, there is a strong divergence between the instruments. The PPS and DiSC indicate mass emissions rising to about 1 mg/s, while the DustTrak and PASS show an emission rate below 0.1 mg/s. Concurrently, the DiSC shows particle size to decrease from ~60 to 16 nm (Figure S6).

This divergence occurs during a portion of the US06 where exhaust temperatures rise to the range of 500–600°C. These temperatures can release sulfur stored on the catalyst and hydrocarbons stored on exhaust system surfaces (Hall and Dickens 2000; Swanson et al. 2009). In addition, they can cause artifacts from release of material deposited on transfer hose walls that carry vehicle exhaust to the dilution tunnel (Maricq et al. 1999). These can then nucleate as they cool after dilution. The lack of photoacoustic response and the sudden decrease in DiSC-reported size suggest that the divergence arises from a nucleation event of semivolatile material.

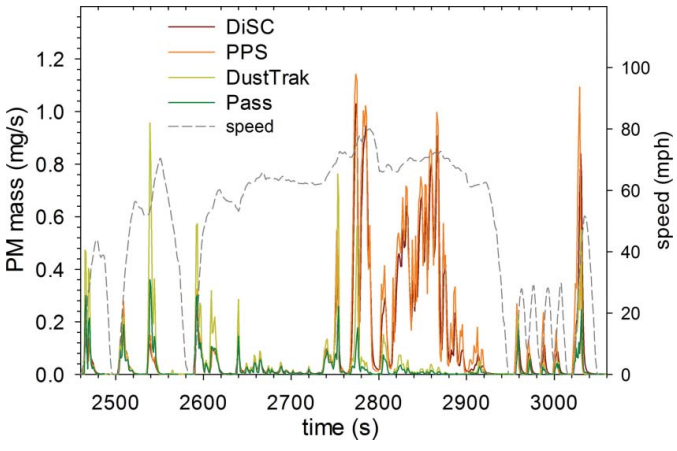

FIG. 4. Divergence in real-time instrument PM readings during US06 drive cycle (DiSC/PPS vs. DustTrak/PASS). Test vehicle is a 2.0 L GTDI. (Color figure available online.)

The DiSC and PPS track each other well because both rely on electrical charging to detect particles. This method depends weakly on particle composition, so both respond to the sudden increase in particles. But the mass emission rate they give in Figure 4 is not quantitatively correct, unless the changes in particle size and density between accumulation and nuclei mode particles are accounted for in the mass calculation by Equation (1). During the ~100 s when nucleation mode particles dominate, the DiSC yields good estimates for their number and size. More generally, if two modes are present, neither DiSC nor PPS can differentiate them. The DustTrak and PASS do not see the nucleation mode. Hydrocarbon droplets do not efficiently absorb light, so are not detected photoacoustically. The DustTrak is also composition dependent, but misses the nucleation mode primarily because of its d^6 size dependence. What this contrast between instruments shows is that the DustTrak, PPS, and DiSC can measure PM mass and number with good accuracy as long as the nature of the PM remains within relatively narrow tolerances. The next section examines in detail how particle size, composition, and charge affect their performance.

Instrument Characterization with Oil and Soot Particles

To compare instrument performance for oil versus soot aerosols, their readings, R_i, are normalized by particle number concentration, N_0, and sample flow rate, F_i, to define response factors

$$\varepsilon_i = \frac{R_i}{F_i N_0}, \qquad [2]$$

with i = DT, PPS, or DiSC. R_{DT} is mass for the DustTrak; thus, ε_{DT} has units mass/particle (note that the DustTrak itself normalizes for flow). $R_i = I_i Q$ for the PPS and DiSC, where I_i is the measured current and $Q = 6.24 \times 10^{18}$ charges/C; hence, ε_i has units charge/particle. As the data below demonstrate, the response factors exhibit power law dependencies on mobility diameter

$$\varepsilon_i = k_i d_m^{\alpha_i}, \qquad [3]$$

parameterized by a scale factor, k_i, and exponent, α_i. These represent "effective" charging efficiencies for the PPS and DISC since they include penetration through the charger.

For polydisperse aerosols, the data are similarly normalized by particle concentration, recorded by SMPS, and sample flow rate (see the online supplemental information). But the breath of size distribution introduces a bias into the measured response factors. Integration of Equation (3) over a lognormal distribution

yields

$$\varepsilon_i = k_i \mu_g^{\alpha_i} e^{\alpha_i^2 (ln\sigma_g)^2/2}, \quad [4]$$

The exponential term arises from the nonlinear response to particle size. In this case, we plot adjusted response factors $\varepsilon_i^* = \varepsilon_i / e^{\alpha_i^2 (ln\sigma_g)^2/2}$ against mobility diameter to maintain consistency with the monodisperse aerosol results.

DustTrak

Figure 5 displays DustTrak response to PAO oil and soot particles. Both are measured using polydisperse aerosols. The oil aerosol data follow a power law regression, where the slope $\alpha_{DT} = 6.02 \pm 0.15$ equals the Rayleigh scattering limit for spherical droplets (DustTrak $\lambda = 780$ nm). Monodisperse oil drops yield the same result but with more noise, owing to the lower particle concentrations.

Changing from oil to soot has a big impact. The soot response is 4–10 times smaller, and the regression exhibits some curvature. The decrease in overall response arises from the difference in the index of refraction between soot and oil. The curvature originates from soot morphology. For small particles, the slope approaches 6, consistent with soot aggregates approaching monomers. At large mobility diameter, the slope decreases, as the increasingly fractal-like soot structure occupies progressively less of the mobility volume.

The DustTrak has a much steeper response to mobility diameter than mass does (dashed lines in Figure 5 with slopes of 3 and 2.3). The response to soot matches the correct mass at about 220 nm, a size near the upper end of exhaust PM, but is about 50 times too small at an engine exhaust particle size of ~70 nm.

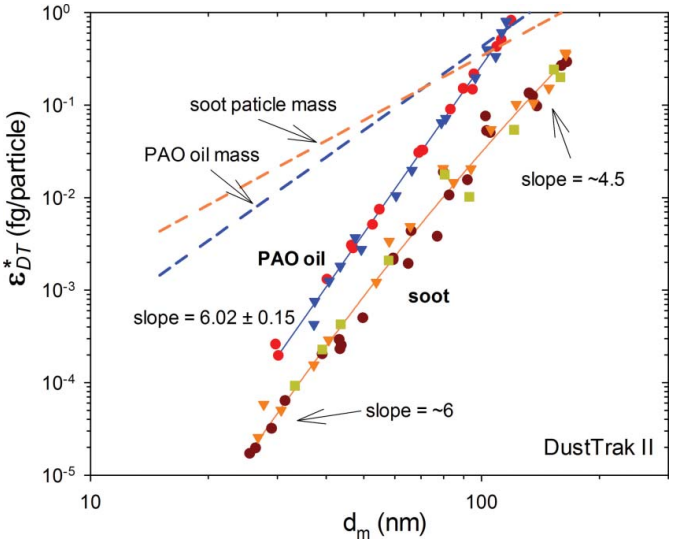

FIG. 5. DustTrak response to PAO oil and soot particles as a function of particle size. Solid lines represent best-fit power law regressions to the data. Dashed lines display oil and soot particle mass dependence versus size. Distinct symbol shape/color represents repeat measurements. (Color figure available online.)

So, why does the DustTrak perform as well as observed on engine exhaust PM? The explanation is that the DustTrak is calibrated against a polydisperse aerosol (Arizona Test Dust), but the adjusted response, $\varepsilon_{DT}{}^*$, plotted in Figure 5 factors out the effect of polydispersity (exponential factor in Equation (4)). For exhaust PM where σ_g is typically 1.7, the unadjusted response is 45 times larger than what is plotted due to the large value of α_{DT}, and this matches soot mass at ~70 nm. It is noteworthy that this unadjusted response to nominally 70-nm particles is dominated by much larger 220-nm particles in the tail of the distribution. The same applies to oil aerosols, but the extent depends on the σ_g involved.

PPS

Figure 6 displays the PPS response to size-selected PAO oil droplets. It is quite different for positive, neutral, and negatively charged particles, an observation that holds also for soot particles, and is independent of air versus nitrogen diluent. This charge dependence originates from the combination of positive corona and escaping charge detection. Particles entering the sensor reach a final state of charge that depends on their size but not their initial charge. This means that a negative particle removes more positive ions (charge) from the corona than a neutral particle when it exits the sensor, whereas a positive particle removes less. The neutral particle response follows a power law regression in mobility diameter, $\alpha_{PPS} = 1.15 \pm 0.03$, which coincides with the average response to +1 and –1 charged particles. This is important, since it validates the use of the PPS for bipolar aerosols such as produced by combustion processes.

The PPS responses to polydisperse oil and soot aerosols are compared in Figure 7. The regression for oil droplets is in very close agreement with the monodisperse data. ε_{PPS} recorded at sample flows from 2.2 and 6.1 L/min collapse onto the same

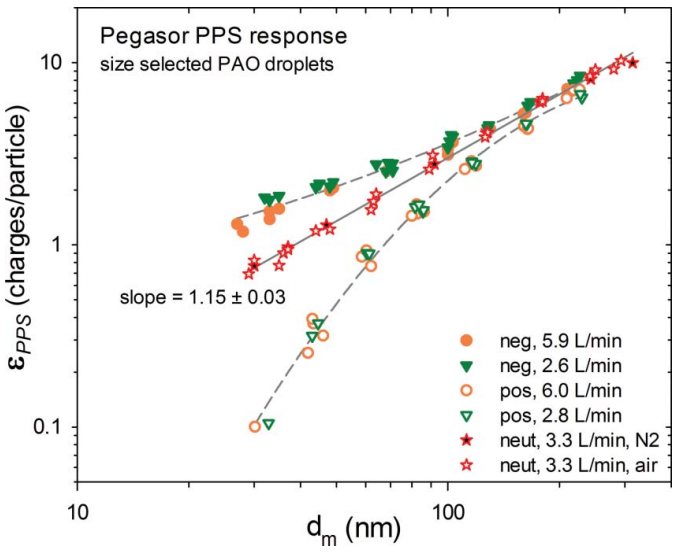

FIG. 6. PPS response to size-selected +1 charge, neutral, and –1 charge oil droplets. (Color figure available online.)

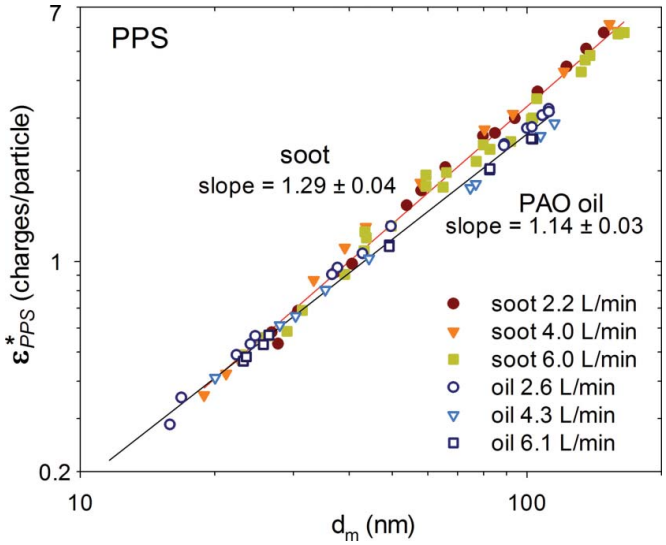

FIG. 7. PPS response to polydisperse PAO oil and soot particles. (Color figure available online.)

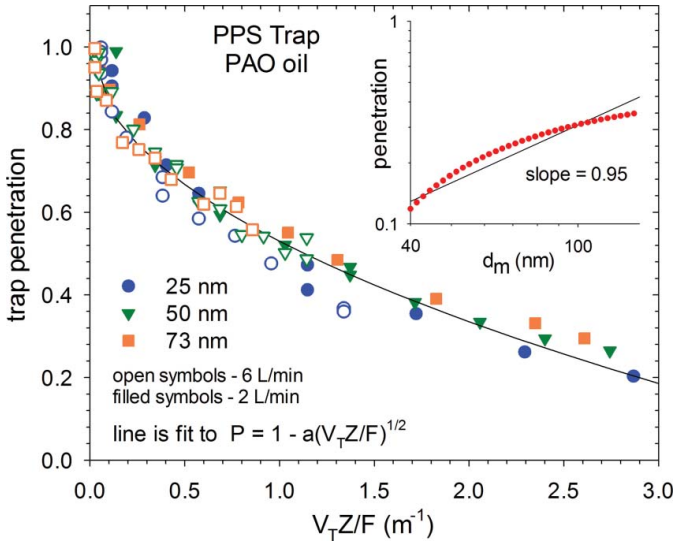

FIG. 8. Particle penetration through PPS trap. Main figure plots data for 25-, 50-, and 73-nm particles at 2 and 6 L/min flow rates through the sensor. Inset shows penetration versus size at $V_{trap} = 800$ V and $F = 2$ L/min. (Color figure available online.)

lines, indicating the PPS responds linearly to flow over this range. At small sizes, where soot particles approach a spherical shape, the PPS responses to oil and soot coincide, implying there is negligible effect of composition. But the regression slope for soot, $\alpha_{PPS} = 1.29 \pm 0.04$, is slightly higher than for oil, a result opposite to the DustTrak. This is an effect of morphology, whereby soot is more efficiently charged because its fractal-like structure has a better ability to spread out electrical charge and reduce repulsion than possible for spherical oil droplets.

The PPS includes an electrical trap with the primary purpose to prevent ions from escaping the corona and producing erroneous particle readings. The trap can also be used to adjust the lower-size cutoff for particle detection. Figure 8 displays oil droplet penetration efficiencies through the trap for three particle sizes at two PPS flow rates, with voltage stepped from 0 V to ~1000 V. As particles flow through the trap, they experience a transverse electrostatic force that induces a drift velocity proportional to $V_T Z$, where V_T is the trap voltage and Z the electrical mobility. Time spent in the trap scales inversely with sample flow rate F; thus, penetration efficiency should scale as $V_T Z/F$. Indeed, Figure 8 shows that the data collapse onto a single curve. The curve's shape suggests that the penetration can be expressed as $P = 1 - a(V_T Z/F)^{\frac{1}{2}}$, which is confirmed by a nonlinear least-square fit ($a = 0.47$ and $R^2 = 0.97$).

Limiting the penetration of small particles can be used to reduce PPS sensitivity to nuclei particles, to filter particles less than 23 nm and thereby mimic solid particle counting, or to enhance robustness of the PPS mass calibration. Regarding the last case, PPS response to soot scales as $d_m^{1.3}$, whereas soot mass scales as $d_m^{2.3}$. If trap penetration followed a d_m^1 dependence, the trap plus soot response would mimic mass. The inset to Figure 8 shows that the trap does not fulfill this dependence globally, but it can be adjusted to approximate the desired response over a limited size region of interest, e.g., a typical diesel soot mode of 70-nm particles. This way, the trap can help compensate for particle size variations from the PPS calibration point during an emission test, but a disadvantage is that it decreases sensitivity.

DiSC

The DiSC simultaneously records two electrical currents, one for particles caught by diffusion and the other for the remaining particles captured by the filter. Figure 9 presents DiSC responses

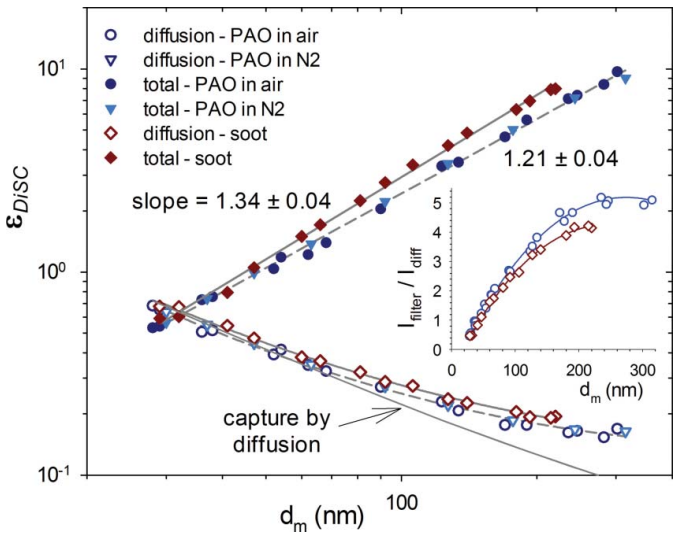

FIG. 9. DiSC response to size-selected oil and soot particles. Solid symbols represent the total response of diffusion screens plus filter (charges/particle). Open symbols show diffusion screen capture efficiency. Inset displays the shift in I_{filter}/I_{diff}, which determines the mean diameter, between soot and oil particles. (Color figure available online.)

to size-selected oil and soot particles. These are the same in air and N_2. Plotted are the charging efficiency, $\varepsilon_{\mathrm{DiSC}} = I_{\mathrm{tot}}/(FN_0)$, and diffusion collection efficiency, $\xi_{\mathrm{diff}} = I_{\mathrm{diff}}/I_{\mathrm{tot}}$. $\varepsilon_{\mathrm{DiSC}}$ exhibits power law regressions for both oil and soot particles. The respective exponents of $\alpha_{\mathrm{DiSC}} = 1.21 \pm 0.04$ and 1.34 ± 0.04 (1.13 ± 0.05 and 1.33 ± 0.13 for polydisperse aerosols in Figure S9) are close to their PPS counterparts. The oil droplet charging efficiency is in good agreement with NaCl particle data ($\varepsilon = 0.015\ d_{\mathrm{m}}^{1.125}$) reported by Fierz et al. (2011). As with the PPS, oil and soot charging efficiencies merge for small particles, but diverge as size increases with soot exhibiting a higher efficiency. If small positively charged particles enter the DiSC with higher charge than achieved by the positive corona, their concentration will be overestimated, whereas negative particles are correctly measured (Figure S11).

The diffusion screen collection efficiency in Figure 9 is well approximated for small particles by $\xi_{\mathrm{diff}} \sim D^{\frac{1}{2}} \sim (C_{\mathrm{c}}/d_{\mathrm{m}})^{\frac{1}{2}}$, where D is the particle diffusion coefficient and C_{c} the Cunningham slip correction. As size increases and diffusion slows, impaction and interception begin to play a role and ξ_{diff} deviates from the $D^{\frac{1}{2}}$ dependence. The deviation is slightly stronger for soot than for oil, as is more clearly evident in the inset, which plots $I_{\mathrm{filter}}/I_{\mathrm{diff}}$ versus d_{m}. This may originate from enhanced interception by the diffusion screens of fractal-like versus spherical particles of the same mobility diameter, as reported for fibrous filters (Kim et al. 2009).

The DiSC calculates particle number concentration and geometric mean diameter assuming a unimodal lognormal size distribution. These are compared with electrometer measurements of number and SMPS size data for monodisperse oil and soot particles in Figure 10 (and polydisperse in Figure S10).

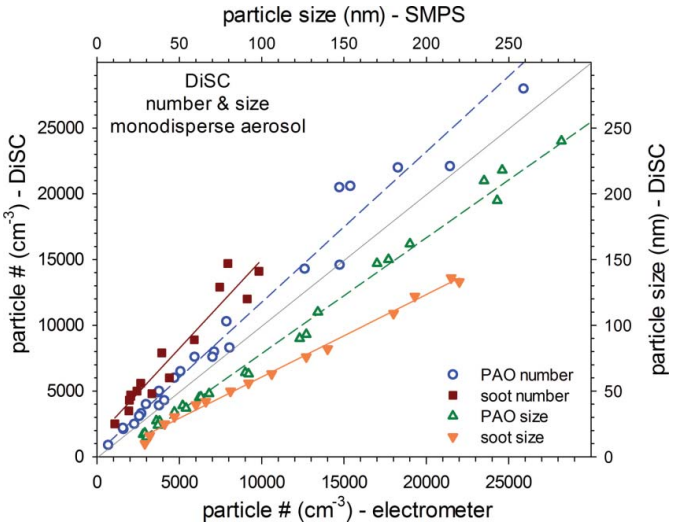

FIG. 10. Comparison of oil and soot particle number from DiSC versus electrometer (left and bottom axes). Comparison of particle size from DiSC with SMPS (right and top axes). DiSC values based on factory calibration. (Color figure available online.)

Number and size regressions for oil fall close to the 1-to-1 line; the DiSC estimate for oil particle number is about 15% high and the size estimate correspondingly low. This possibly originates from variability in α_{DiSC} (factory calibrated value is 1.02), but it may also arise from the $\sigma_{\mathrm{g}} = 1.9$ assumed in calibration versus the ~1.07 monodisperse and ~1.5 polydisperse test aerosols. The soot results deviate more markedly. Since in this case σ_{g} is the same as for oil, the likely explanations are the steeper charging efficiency, $\alpha_{\mathrm{DiSC}} = 1.34$, and enhanced interception by the diffusion screens. For application to engine exhaust, a simple recalibration to soot particles, such as in Figure 9, will correct the number and size data.

DISCUSSION

There is no simple answer to the question of how suitable these monitors are for engine exhaust PM measurement. All three perform well over the FTP test for the GTDI vehicles tested, where PM morphology and composition remain relatively constant. This ceases during some US06 tests when the nature of the PM changes. This by itself does not mean that one monitor is good and another poor; PM is too complex a substance to expect a simple one- or two-dimensional measurement to adequately characterize. Instead, the answer depends on a benefit/drawback compromise, which varies with intended application.

As Figure 5 demonstrates, DustTrak response is composition dependent and not proportional to mass. This is consistent with the observations by Moosmüller et al. (2001), that its calibration varies with vehicle type. On the other hand, for the fixed vehicle type in the present study, the DustTrak yields PM mass that is in good agreement with the regulatory method (within ~25%). It also proved useful in the Kansas City in-use gasoline vehicle study to augment filter measurements with real-time PM emissions data (US EPA 2008). The DustTrak could serve a useful role in monitoring long or repeated tests of the same engine/fuel type, especially in field testing or on-board applications as long as the PM is dominated by soot or semivolatiles, but does not switch between the two. Drawbacks are that it is insensitive to nuclei mode particles, if this is of interest, and it is susceptible to interference from large particles, e.g., resuspended particles from exhaust pipe or sampling system walls if these are not removed with a 2.5- or 1-μm impactor at the inlet.

The PPS and DiSC charging efficiencies are similar to those previously reported for diffusion chargers (Ntziachristos et al. 2004; Jung and Kittelson 2005). These devices exhibit the same small but systematically higher charging efficiency of soot agglomerates relative to spherical particles noted in the previous work. But this sensitivity to particle composition, as well as size, remains much smaller than for the DustTrak. This, and a size dependence intermediate between mass and number, should make diffusion charging an attractive method for PM monitoring. There are, however, some disadvantages. One

is the susceptibility to fouling, where soot deposits on the corona needle decrease charging efficiency. Another, in the case of the PPS, is relating the measured current to the common metrics of number or mass without prior knowledge of mean diameter.

The PPS and DiSC provide some attractive features for exhaust PM measurement. The PPS is designed with vehicle testing in mind (Lanki et al. 2011); the corona needle is protected by the ejector flow used to draw in the exhaust sample, and the charged particles are sensed with no need for contact with the sensor, e.g., collection by filter. The scope of the present work did not include investigating durability, but the PPS performed satisfactorily in a study of its effectiveness in detecting damaged diesel particulate filters (Ntziachristos et al. 2011). The electrical trap may allow the PPS to partially address the issue of reporting PM emissions in units of mass. Thus, it should be feasible to choose a mass calibration (mean diameter/trap voltage) suitable for a particular engine type and then use the PPS to monitor PM emissions as the engine undergoes testing/development. It would alert the user to sudden changes in the nature of the aerosol, such as the appearance of a nucleation mode, even if the reported mass or number during such changes is not quantitative.

The DiSC is not designed for motor vehicle applications, but can be used to measure diluted exhaust. The added dimension of the diffusion stage provides a key benefit; namely it adds the measurement of mean diameter, which then provides sufficient information to estimate particle number or PM mass. This feature distinguishes it from the PPS, but otherwise, the performance in terms of sensitivity and size and composition dependence is the same.

The upcoming LEV III regulations limit PM emissions to 3 mg/mile. As seen in Figures 2, S3, and S4, all three monitors have good signal-to-noise ratio in this emission range, even with diluted exhaust. The values they report are consistent with gravimetric PM and exhibit lower variability; however, mass determination requires additional input in the form of particle effective density. The sensitivity looks to be sufficient for a 1 mg/mile standard, but there are a number of issues, including PM composition at these levels and whether a filter-based operational definition of PM remains meaningful, that require further study.

REFERENCES

Akard, M., Oestergaard, K., Chase, R., Richert, J., Fukushima, H., and Adachi, M. (2004). Comparison of an Alternative Particulate Mass Measurement with Advanced Microbalance Analysis, SAE Technical Paper 2004-01-0589. SAE, Warrendale, PA.

Bukowiecki, N., Kittelson, D. B., Watts, W. F., Burtscher, H., Weingartner, E., and Baltensperger, U. (2002). Real-Time Characterization of Ultrafine and Accumulation Mode Particles in Ambient Combustion Aerosols, *J. Aerosol Sci.,* 33:1139–1154.

Burtscher, H. (2005). Physical Characterization of Particulate Emissions from Diesel Engines: A Review, *J. Aerosol Sci.,* 36:896–932.

Cauda, E. G., Ku, B. K., Miller, A. L., and Barone, T. L. (2012). Toward Developing a New Occupational Exposure Metric Approach for Characterization of Diesel Aerosols. *Aerosol Sci. Technol.,* 46:1370–1381.

Fierz, M., Burtscher, H., Steigmeier, P., and Kasper, M. (2008a). Field Measurement of Particle Size and Number Concentration with the Diffusion Size Classifier (Disc). SAE Technical Paper, 2008-01-1179. SAE, Warrendale, PA.

Fierz, M., Houle, C., Steigmeier, P., and Burtscher, H. (2011). Design, Calibration, and Field Performance of a Miniature Diffusion Size Classifier. *Aerosol Sci. Technol.,* 45:1–10.

Fierz, M., Weimer, S., and Burtscher, H. (2008b). Design and Performance of an Optimized Electrical Diffusion Battery. *J. Aerosol Sci.,* 40:152–163.

Giechaskiel, B., Mamakos, A., Andersson, J., Dilara, P., Martini, G., Schindler, W., et al. (2012). Measurement of Automotive Non-Volatile Particle Number Emissions Within the European Legislative Framework: A Review. *Aerosol Sci. Technol.,* 46:719–749.

Hall, D., and Dickens, C. (2000). Measurement of the Numbers of Emitted Gasoline Particles: Genuine or Artefact? SAE Technical Paper 2000-01-2957. SAE, Warrendale, PA.

Harris, S. J., and Maricq, M. M. (2001). Signature Size Distributions for Diesel and Gasoline Engine Exhaust Particulate Matter. *J. Aerosol Sci.,* 32:749–764.

Homan, H. S. (1985). Conversion Factors Among Smoke Measurements. SAE Technical Paper 850267. SAE, Warrendale, PA.

Jung, H., and Kittelson, D. B. (2005). Characterization of Aerosol Surface Instruments in Transition Regime. *Aerosol Sci. Technol.,* 39:902–911.

Khalek, I. (2007). 2007 Diesel Particulate Measurement Research, Phase 3 Final Report, CRC Report No. E-66–3. Available from: http://www.crcao.org/publications/emissions/index.html

Kim, S. C., Wang, J., Emery, M. S., Shin, W. G., Mulholland, G. W., and Pui, D. Y. H. (2009). Structural Property Effect of Nanoparticle Agglomerates on Particle Penetration Through Fibrous Filter. *Aerosol Sci. Technol.,* 43:344–355.

Lanki, T., Tikkanen, J., Janka, K., Taimisto, P., and Lehtimäki, M. (2011). An Electrical Sensor for Long-Term Monitoring of Ultrafine Particles in Workplaces. *J. Physics Conf. Series*, 304:012013.

Lehmann, U., Niemelä, V., and Mohr, M. (2004). New Method for Time-Resolved Diesel Engine Exhaust Particle Mass Measurement. *Environ. Sci. Technol.* 38:5704–5711.

Lehtimäki, M (1983). Modified Aerosol Detector, In *Aerosols in Mining and Industrial Work Environment 3*, V. A. Marple and B. Y. H. Liu, eds., Ann Arbor Science Publishers, Ann Arbor, MI, pp. 1135–1143.

Lee, S.-C., Guo, H., Li, W.-M., and Chan, L.-Y. (2002). Inter-Comparison of Air Pollutant Concentrations in Different Indoor Environments in Hong Kong. *Atmos. Environ.,* 36:1929–1940.

Liebowitz, B., and Hansen, T. A. (2011). Evaluation of On-Board Real-Time Particulate Emissions Measurement Technologies, Final Report. New York State Energy Research and Development Authority, Albany, NY.

Linke, M., Schindler, W., and Vizeu de Almeida, W. (2004). A New Device for Transient Measurement of Ultralow Soot Emissions. SAE Technical Paper 2004-01-3267. SAE, Warrendale, PA.

Maricq, M. M., Chase, R. E., Podsiadlik, D. H., and Vogt, R. (1999). Vehicle Exhaust Particle Size Distributions: A Comparison of Tailpipe and Dilution Tunnel Measurements. SAE Technical Paper, 1999-01-1461. SAE, Warrendale, PA.

Maricq, M. M., and Xu, N. (2004). The Effective Density and Fractal Dimension of Soot Particles from Premixed Flames and Motor Vehicle Exhaust. *J. Aerosol Sci.,* 35:1251–1274.

Mohr, M., Lehmann, U., and Rutter, J. (2005). Comparison of Mass-Based and Non-Mass-Based Particle Measurement Systems for Ultra-Low

Emissions from Automotive Sources. *Environ. Sci. Technol.,* 39:2229–2238.

Moosmüller, H., Arnott, W. P., Rogers, C. F., Bowen, J. L., Gillies, J. A., Pierson, W. R., et al. (2001). Time Resolved Characterization of Diesel Particulate Emissions. 1. Instruments for Particle Mass Measurements. *Environ. Sci. Technol.,* 35:781–787.

Ntziachristos, L., Fragkiadoulakis, P., Samaras, Z., Janka, K., Tikkanen, J. (2011). Exhaust Particle Sensor for OBD Application, SAE Technical Paper 2011-01-0626. SAE, Warrendale, PA.

Ntziachristos, L, Giechaskiel, B, Ristimäki, J, and Keskinen, J. (2004). Use of a Corona Charger for the Characterization of Automotive Exhaust Aerosol. *J Aerosol Sci.,* 35:943–963

Seaton, A., Cherrie, J., Dennekamp, M., Donaldson, K., Hurley, J. F., and Tran, C. L. (2004). The London Underground: Dust and Hazards to Health. *Occup. Environ. Med.,* 62:355–362.

Swanson, J., Kittelson, D., Watts, W., Gladis, D., and Twigg, M. (2009). Influence of Storage and Release on Particle Emissions from New and Used CRTs. *Atmospheric Environ.,* 43:3998–4004.

United States Environmental Protection Agency. (2008). Analysis of Particulate Matter Emissions from Light-Duty Gasoline Vehicles in Kansas City. Available from: http://www.epa.gov/oms/emission-factors-research/420r08010.pdf

United States Environmental Protection Agency. (2011). Code of Federal Regulations, Title 40—Protection of the Environment, Part 1065—Engine Testing Procedures. Available from: http://ecfr.gpoaccess.gov/cgi/t/text/text-idx?c=ecfr&tpl=/ecfrbrowse/Title40/40cfr1065_main_02.tpl

Wiesner, M. R., Lowry, G. V., Alvarez, P., Dionysiou, D., and Biswas, P. (2006). Assessing the Risks of Manufactured Nanomaterials. *Environ. Sci. Technol.*, 40:4336–4345.